Electronic Supplementary Material (ESI) for Sustainable Energy & Fuels.


# Electronic Supplementary Information

## $Sm^{3+}$ rare-earth doping in non-noble metal oxide –$WO_3$ grown on carbon cloth fibre as a bifunctional electrocatalyst for high-performance water electrolysis.

**R. Rajalakshmi, C. Viswanathan and N. Ponpandian***

Department of Nanosience and Technology, Bharathiar University, Coimbatore 641 046, India

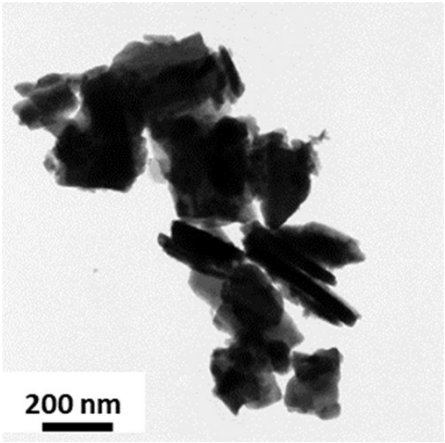


Figure S1. TEM image of Sm 5% doped $WO_3$ electrocatalyst representing rod and particle morphologies.

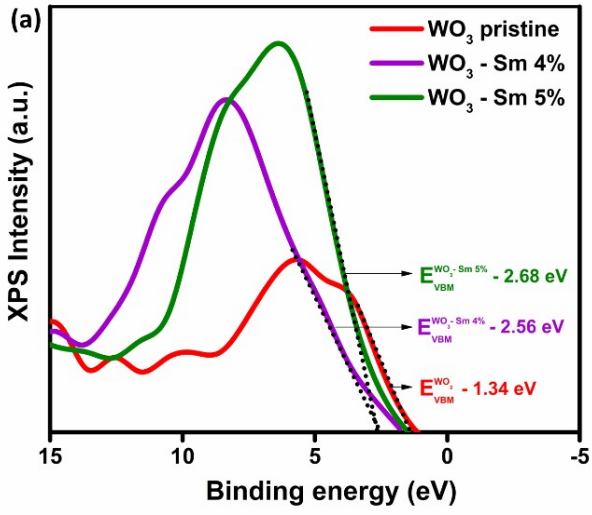


Figure S2. The valence band (VB) edges of pristine $WO_3$, $WO_3$ - Sm 4%, and $WO_3$ - Sm 4% electrocatalysts.

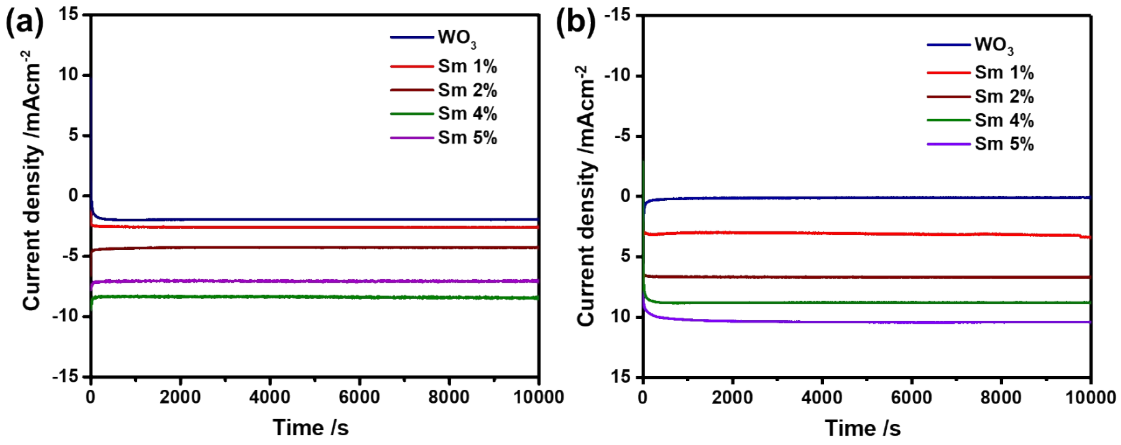


Figure S3. Chronoamperometry curves recorded for all the prepared electrocatalysts of pure and Sm doped $WO_3$ for 10,000 s recorded for (a) HER and (b) OER.

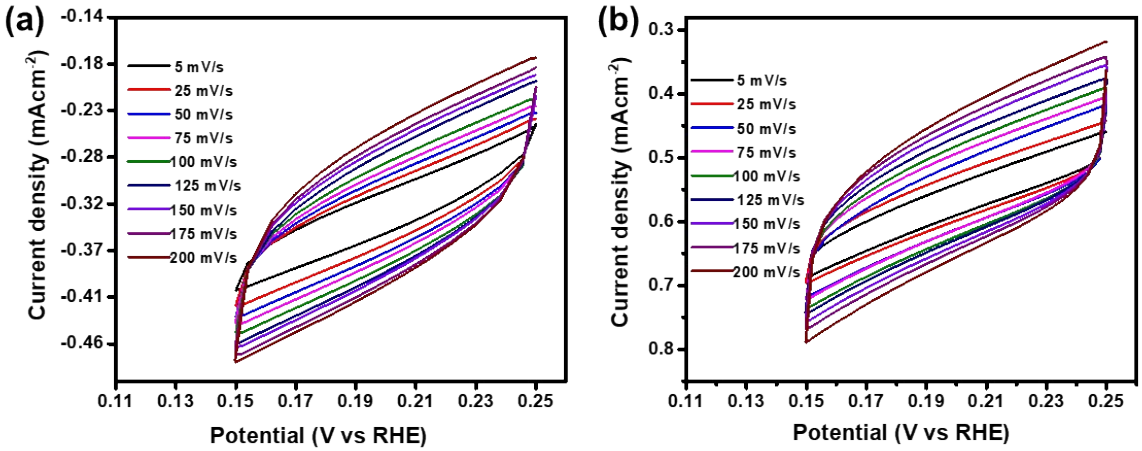


Figure S4. Cyclic voltammograms recorded in the non-Ohmic region of (a) $WO_3$ – Sm 4% and (b) $WO_3$ – Sm 5% electrocatalysts.

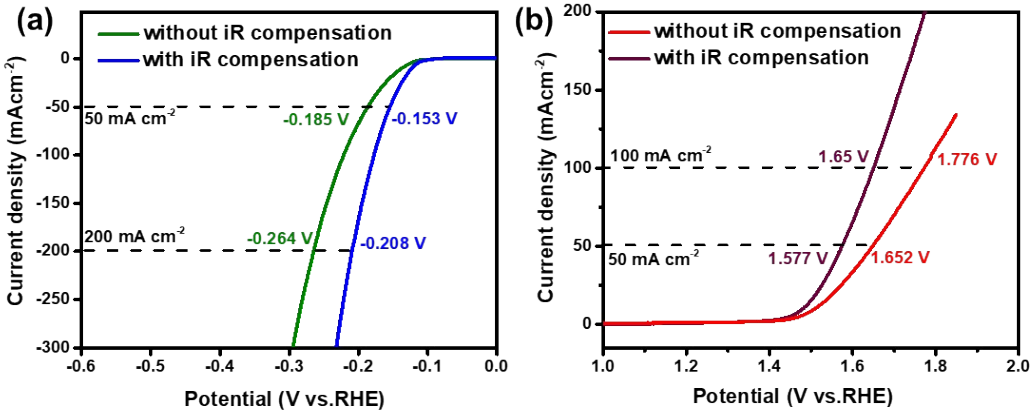

Figure S5. The LSV polarization curves of (a) Sm 4% doped $WO_3$ electrocatalyst with and without iR compensation for HER and (b) Sm 5% doped $WO_3$ electrocatalyst with and without iR compensation for OER.

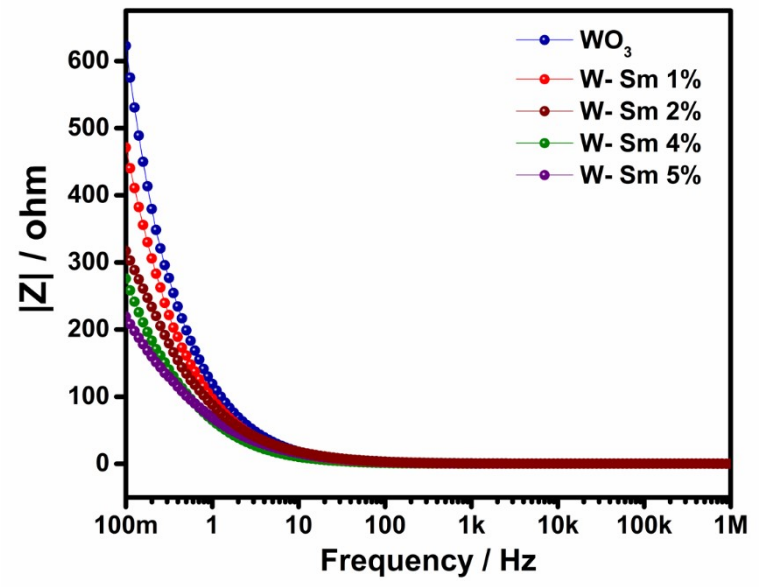


Figure S6. The Bode impedance plot obtained from the electrochemical impedance spectroscopy for all the electrocatalyst of $WO_3$ and its Sm doped constituent.

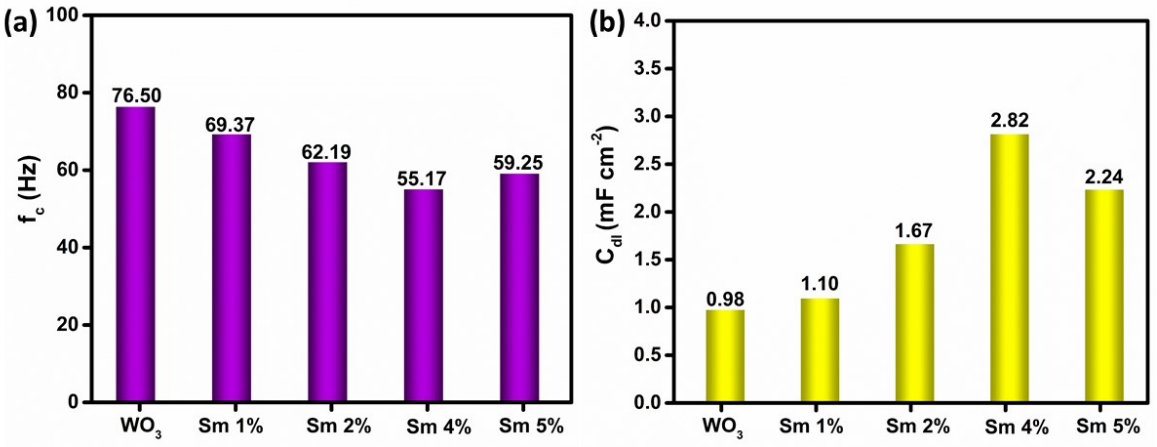


Figure S7. Comparison of (a) cut-off frequency ($f_c$) in Hz with the (b) electrochemical active surface area ($C_{dl}$) in mF $cm^{-2}$ of all the synthesized electrocatalysts.

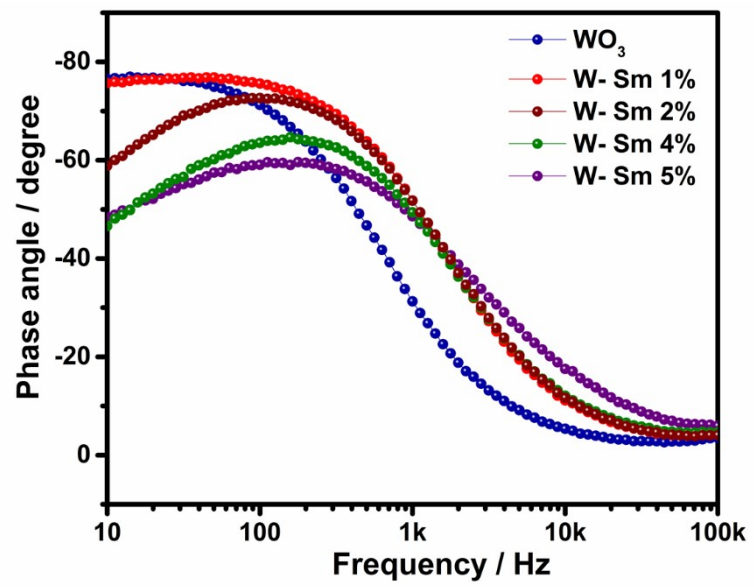


Figure S8. (a) Bode phase angle plot of all the synthesized $WO_3$ electrocatalysts obtained from the electrochemical impedance spectroscopy.

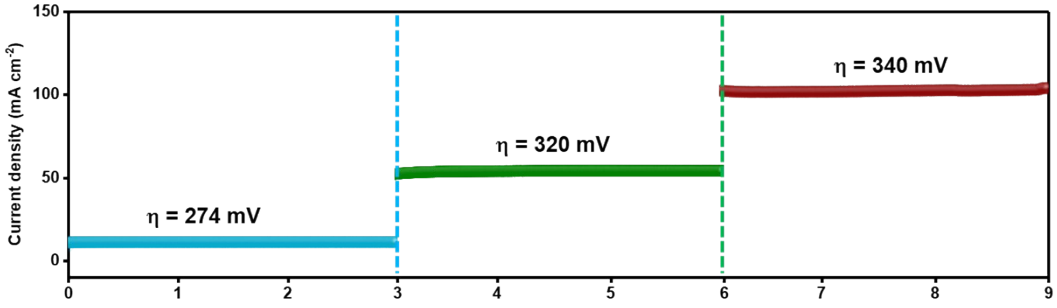


Figure S9. Prolonged potentiostatic electrolysis with Sm 5% doped $WO_3$ electrocatalyst for OER varying the onset potential in different intervals of time.

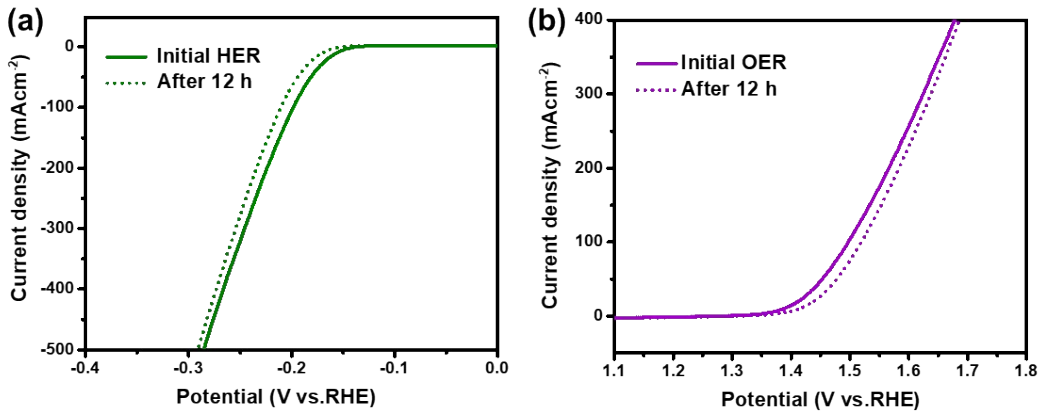


Figure S10. a) LSV measurements of HER screened at 5 mV $s^{-1}$ on $WO_3$ – Sm 4% before and after potentiostatic electrolysis, (b) LSV measurements of OER screened at 5 mV $s^{-1}$ on $WO_3$ – Sm 5% electrocatalyst before and after the prolonged potentiostatic electrolysis.

Table S1. The calculated mass loading of electrochemical activated $WO_3$ – Sm 4% for HER and $WO_3$ – Sm 5% for OER on carbon cloth fibre (CC) substrate.

| Sample code | Mass loading ($mg/cm^2$) |
|---|---|
| | 0.5M $H_2SO_4$ |
| CC@$WO_3$ – Sm 4% | 3.67 ± 0.27 |
| CC@$WO_3$ – Sm 5% | 3.34 ± 0.26 |

Table S2. The comparison of HER activity between the Sm 4% doped $WO_3$ catalyst and other reported electrocatalysts of $WO_3$ derived from Fig 13c.

| S. No | Electrocatalyst | Overpotential (η) @ 10 mA $cm^{-2}$ (mV) | Tafel slope ( mV $dec^{-1}$) | Reference |
|---|---|---|---|---|
| 1. | Zeolite/WO3 | 138 | 500 | [1] |
| 2. | Mn-WO3 | 63 | 61 | [2] |

| | | | | |
|---|---|---|---|---|
| 3. | $WO_3$-x@NC | 37 | 96 | [3] |
| 4. | G/$WS_2$/$WO_3$ | 90 | 100 | [4] |
| 5. | $WSe_2$/$WO_3$-y | 58.2 | 185 | [5] |
| 6. | Pd@$WO_3$ | 95 | 287 | [6] |
| 7. | Meso-$WO_{2.83}$ | 87 | 225 | [7] |
| 8. | $WO_3$/NPRGO | 115 | 40 | [8] |
| 9. | $WO_3$/C@CoO | 61 | 42 | [9] |
| 10. | Pt/$WO_3$ | 121 | 150 | [10] |
| 11. | $CoSe_2$/$WSe_2$/$WO_3$@CC | 68 | 97 | [11] |
| 12. | $WS_2$/$WO_3$ | 50 | 395 | [12] |
| 13. | $WO_x$ Nws/N-rGO | 38.2 | 40 | [13] |
| 14. | Ta-$WO_3$ | 65 | 470 | [14] |
| 15. | Fe-$WO_x$P/rGO | 42 | 54.6 | [15] |
| 16. | $WO_3$ – Sm 4% | 67 | 135 | This work |
| 17. | CC@$WO_3$ – Sm 4% | 54 | 157 | This work |

Table S3. The comparison of OER activity between the Sm 5% doped $WO_3$ catalyst and other reported electrocatalysts of $WO_3$ obtained from Fig 13d.

| S. No | Electrocatalyst | Overpotential (η) @ 10 mA $cm^{-2}$ (mV) | Tafel slope ( mV $dec^{-1}$) | Reference |
|---|---|---|---|---|
| 1. | $WO_3$-Vo (oxygen vacancies) | 183.3 | 590 | [16] |
| 2. | $IrO_2$/$WO_3$ | 65 | 420 | [17] |
| 3. | $H_x$-$WO_3$ | 134 | 110 | [18] |
| 4. | $SrCo_{0.4}Fe_{0.2}W_{0.4}O_{3-\delta}$ | 104 | 296 | [19] |
| 5. | $WO_{3-x}$@NC | 86 | 306 | [3] |
| 6. | Pd@$WO_3$ | 62.8 | 113 | [6] |
| 7. | $WO_3$ – Sm 5% | 102 | 146 | This work |
| 8. | CC@$WO_3$ – Sm 5% | 90 | 138 | This work |

Table S4: Comparison of water-splitting performances for CC@$WO_3$-Sm 4% and CC@$WO_3$-Sm 5% with reported bifunctional electrocatalysts in the acidic media.

| S.No | Electrocatalyst | Substrate | Potential | Refs. |
|---|---|---|---|---|
| 1. | $CoS_2$ nanotube | Carbon cloth | 1.67 at 10 mA $cm^{-2}$ | Nanoscale Horiz. 2017, 2, 342. |
| 2. | Ni/$Mo_2C$ | Carbon cloth | 1.66 at 10 mA $cm^{-2}$ | Chem. Sci. 2018, 8, 968. |
| 3. | P-$Co_3O4$ | Ni foam | 1.63 at 10 mA $cm^{-2}$ | ACS Catal. 2018, 8, 2236. |
| 4. | E-Mo-NiCoP\|\| MoNiCoP | Carbon cloth | 1.61 at 10 mA $cm^{-2}$ | Nano-Micro Letters, 2019,11, 55 |
| 5. | $NiMoP_2$ nanowires | Carbon cloth | 1.67 at 10 mA $cm^{-2}$ | J. Mater. Chem. A 2020, 5, 7191. |
| 6. | $NiCo_2P_2$/graphene quantum dot | Ti mesh | 1.61 at 10 mA $cm^{-2}$ | Nano Energy 2020, 48, 284. |
| 7. | FeCoP ultrathin arrays | Ni foam | 1.60 at 10 mA $cm^{-2}$ | Nano Energy 2021, 41, 583. |
| 8. | N-$NiMoO_4$/$NiS_2$ | Carbon cloth | 1.60 at 10 mA $cm^{-2}$ | Adv. Funct. Mater. 2021, 29, 1805298. |
| 9. | CC@$WO_3$-Sm 4% \|\| CC@$WO_3$-Sm 5% | Carbon cloth | 1.60 V at 10 mA $cm^{-2}$ | This work |

Reference


[1] S.F. Anis, R. Hashaikeh, Electrochemical water splitting using nano-zeolite Y supported tungsten oxide electrocatalysts, J. Nanoparticle Res. 20 (2018). doi:10.1007/s11051-018-4153-2.

[2] S. Chandrasekaran, P. Zhang, F. Peng, C. Bowen, J. Huo, L. Deng, Tailoring the geometric and electronic structure of tungsten oxide with manganese or vanadium doping toward highly efficient electrochemical and photoelectrochemical water splitting, J. Mater. Chem. A. 7 (2019) 6161–6172. doi:10.1039/c8ta12238e.

[3] J. Chen, H. Yang, X. Sang, Z. Su, D. Li, Q. Wang, Oxygen vacancy rich tungsten oxide with nitrogen doped mesoporous carbon as matrix for overall water splitting and 4-nitrophenol reductive removal, Solid State Sci. 83 (2018) 23–30. doi:10.1016/j.solidstatesciences.2018.06.010.

[4] Y. Chen, R. Ren, Z. Wen, S. Ci, J. Chang, S. Mao, J. Chen, Superior electrocatalysis for hydrogen evolution with crumpled graphene/tungsten disulfide/tungsten trioxide ternary nanohybrids, Nano Energy. 47 (2018) 66–73. doi:10.1016/j.nanoen.2018.02.023.

[5] V.Y. Fominski, S.N. Grigoriev, R.I. Romanov, M.A. Volosova, A.I. Grunin, G.D. Teterina, The formation of a hybrid structure from tungsten selenide and oxide plates for a hydrogen-evolution electrocatalyst, Tech. Phys. Lett. 42 (2016) 555–558. doi:10.1134/S1063785016060055.

[6] R. Choudhary, S. Patra, R. Madhuri, P.K. Sharma, Cow Dung Derived PdNPs@$WO_3$ Porous Carbon Nanodiscs as Trifunctional Catalysts for Design of Zinc-Air Batteries and Overall Water Splitting, ACS Sustain. Chem. Eng. 5 (2017) 9735–9748. doi:10.1021/acssuschemeng.7b01541.

[7] H. Cheng, M. Klapproth, A. Sagaltchik, S. Li, A. Thomas, Ordered mesoporous $WO_{2.83}$: Selective reduction synthesis, exceptional localized surface plasmon resonance and enhanced hydrogen evolution reaction activity, J. Mater. Chem. A. 6 (2018) 2249–2256. doi:10.1039/c7ta09579a.

[8] G. Hu, J. Li, P. Liu, X. Zhu, X. Li, R.N. Ali, B. Xiang, Enhanced electrocatalytic activity of $WO_3$ @NPRGO composite in a hydrogen evolution reaction, Appl. Surf. Sci. 463 (2019) 275–282. doi:10.1016/j.apsusc.2018.08.227.

[9] Y. Lv, Y. Liu, C. Chen, T. Wang, M. Zhang, Octopus tentacles-like $WO_3$/C@CoO as high property and long life-time electrocatalyst for hydrogen evolution reaction, Electrochim. Acta. 281 (2018) 1–8. doi:10.1016/j.electacta.2018.05.145.

[10] H. Tian, X. Cui, L. Zeng, L. Su, Y. Song, J. Shi, Oxygen vacancy-assisted hydrogen evolution reaction of the Pt/$WO_3$ electrocatalyst, J. Mater. Chem. A. 7 (2019) 6285–6293. doi:10.1039/c8ta12219a.

[11] Y. Lv, Y. Liu, Y. Liu, Z. Chen, M. Zhang, $CoSe_2$/$WSe_2$/$WO_3$ hybrid nanowires on

carbon cloth for efficient hydrogen evolution reaction, J. Alloys Compd. 768 (2018) 889–895. doi:10.1016/j.jallcom.2018.07.285.

[12] X. Shang, Y. Rao, S.S. Lu, B. Dong, L.M. Zhang, X.H. Liu, X. Li, Y.R. Liu, Y.M. Chai, C.G. Liu, Novel WS2/WO3 heterostructured nanosheets as efficient electrocatalyst for hydrogen evolution reaction, Mater. Chem. Phys. 197 (2017) 123–128. doi:10.1016/j.matchemphys.2017.05.027.

[13] T.H. Wondimu, G.C. Chen, H.Y. Chen, D.M. Kabtamu, A.W. Bayeh, K.C. Wang, H.C. Huang, C.H. Wang, High catalytic activity of oxygen-vacancy-rich tungsten oxide nanowires supported by nitrogen-doped reduced graphene oxide for the hydrogen evolution reaction, J. Mater. Chem. A. 6 (2018) 19767–19774. doi:10.1039/c8ta07000h.

[14] X. Xie, W. Mu, X. Li, H. Wei, Y. Jian, Q. Yu, R. Zhang, K. Lv, H. Tang, S. Luo, Incorporation of tantalum ions enhances the electrocatalytic activity of hexagonal $WO_3$ nanowires for hydrogen evolution reaction, Electrochim. Acta. 134 (2014) 201–208. doi:10.1016/j.electacta.2014.04.122.

[15] T.H. Wondimu, G.C. Chen, D.M. Kabtamu, H.Y. Chen, A.W. Bayeh, H.C. Huang, C.H. Wang, Highly efficient and durable phosphine reduced iron-doped tungsten oxide/reduced graphene oxide nanocomposites for the hydrogen evolution reaction, Int. J. Hydrogen Energy. 43 (2018) 6481–6490. doi:10.1016/j.ijhydene.2018.02.080.

[16] H. Liang, Z. Cao, C. Xia, F. Ming, W. Zhang, A.-H. Emwas, L. Cavallo, H.N. Alshareef, Tungsten Blue Oxide as a Reusable Electrocatalyst for Acidic Water Oxidation by Plasma-Induced Vacancy Engineering, (n.d.). doi:10.31635/ccschem.020.202000325.

[17] M. Tariq, W.Q. Zaman, Y. Wu, A. Nabi, Z. Abbas, W. Iqbal, W. Sun, Z. Hao, Z.H. Zhou, L. Cao, J. Yang, Facile synthesis of $IrO_2$ nanoparticles decorated @ $WO_3$ as mixed oxide composite for outperformed oxygen evolution reaction, Int. J. Hydrogen Energy. 44 (2019) 31082–31093. doi:10.1016/j.ijhydene.2019.10.013.

[18] A.G. Breuhaus-Alvarez, J.L. Dimeglio, J.J. Cooper, C.R. Lhermitte, B.M. Bartlett, Kinetics and Faradaic Efficiency of Oxygen Evolution on Reduced $H_x$ $WO_3$ Photoelectrodes, J. Phys. Chem. C. 123 (2019) 1142–1150. doi:10.1021/acs.jpcc.8b11777.

[19] G. Chen, Z. Hu, Y. Zhu, Z.G. Chen, Y. Zhong, H.J. Lin, C. Te Chen, L.H. Tjeng, W. Zhou, Z. Shao, Ultrahigh-performance tungsten-doped perovskites for the oxygen evolution reaction, J. Mater. Chem. A. 6 (2018) 9854–9859. doi:10.1039/c8ta02864h.